TRANSPARENT ZNO/GLASS SURFACE ACOUSTIC WAVE DEVICES WITH ALUMINUM DOPED ZNO ELECTRODE

Jian Zhou[1], Xuezhong Wu[1,], Dingbang Xiao[1],Hao Jin[2], Shurong Dong[2], Yongqing Fu[3], and Jikui Luo[2]*
[1] National University of Defense Technology, Changsha, China
[2]Zhejiang University, Hangzhou, China
[3]University of Northumbria, Newcastle upon Tyne, UK

ABSTRACT

This paper reports the fabrication of transparent SAW resonators using AZO as the transparent electrodes. Transparent SAW resonators exhibited two types of wave modes: Rayleigh and Sezawa waves, and signal amplitudes up to 25 dB were obtained with the transparency above 80%. The series resistance effect of the AZO film electrode on the performance of transparent SAW devices have been systematically investigated and results show that the series resistance should be lower than 10 Ω/sq. Temperature sensing showed the transparent SAW device has a temperature coefficient of frequency of ~45 ppm/K. The transparent devices have also demonstrated their ability to induce a strong acoustic streaming with a streaming velocity up to 2.27 cm/s. This research opened a door for further exploration of the SAW devices in transparent electronics such as transparent microfluidics and sensors.

INTRODUCTION

Transparent electronics (also called invisible electronics) has attracted great attention in recent years due to their great potential to make significant commercial impact in variety of areas. Great effort has been made to develop various transparent electronic devices and systems such as transparent thin-film transistors, photovoltaic cells, electronic circuits, displays, sensors, solar cells, and electro-optic devices etc. [1-4]. However, there are a few studies on the transparent surface acoustic wave (SAW) resonators.

SAW resonators are one of the building blocks of electronic devices with widespread applications in communications, micro-sensors, microfluidics and lab-on-a-chip [5-7]. If SAW devices can be made as transparent devices, they could have found widespread and new applications. They can be used as invisible wireless RFIDs and SAW sensor arrays on windows of cars and offices, and on screens of eyeglasses, helmet and other electronic gadgets to monitor environmental conditions such as pressure, temperature as well as to detect biochemical molecules associated with air pollution and biological attachment.

Most of the current SAW devices are typically made on piezoelectric bulk materials or thin films deposited on solid substrates, consisting of a pair of interdigitated electrodes (IDT) which are normally made of metals such as Al and Au. Therefore, the so-made SAW devices are opaque and visible. In this paper, we report the transparent SAW devices made on ZnO/glass substrates using transparent oxide semiconductor as the IDT electrodes, and demonstrate their high transmission performance, yet with transparency above 80%.

EXPERIMENTAL

In this work, aluminum doped ZnO (AZO) was chosen as the IDT material due to its high electrical conductivity and optical transmittance, and transparency to most of visible light owing to the wide optical band gap of 3.3 eV. [8-12]. The AZO was deposited using a home-made DC magnetron sputtering system with a AZO target (ZnO 98 wt.%: Al_2O_3 2 wt.%,) with a diameter of 50 mm. The base pressure of chamber was 1×10^4 Pa before deposition. The distance between the target and substrate was fixed at 70 mm. The effects of deposition conditions such as the pressure on the properties of the AZO films were investigated.

The crystalline structure and crystal orientation of the films were analyzed by X-ray diffraction (XRD-6000, JAPAN) using Cu-K_α radiation and a scanned range of 2θ =20°~70°. The degree of c-axis crystallization was examined by the full-width at half maximum (FWHM) of the AZO (0002) diffraction peak. Crystallite grain sizes were calculated from the Debye–Scherrer formula: $D= K\lambda/(\beta\cos\theta)$, where K is the shape factor of the average crystallite with a value of 0.94, λ the X-ray wavelength (1.5405 Å for Cu target), β the FWHM in radians, θ the Bragg angle, and D the mean crystallite gain size normal to diffracting planes. For cross-sectional structural analysis, a Scanning Electron Microscope (SEM, S4800, HITACHI Company, JAPAN) was used. The resistivity of the AZO layers was measured using the Van de Paul Hall effect measurement. Optical transmittance of the AZO films measured using a UV/visible spectrometer (UV756).

SAW devices were made on 2-inch Corning glass 2318 substrates of 1.1 mm thick, with ZnO thin films as the piezoelectric layer which were deposited using a direct-current (DC) reactive magnetron sputtering system. The optimal deposition conditions of the ZnO film were used: substrate temperature of 100 °C , deposition pressure of 2 Pa, sputtering power of 200 W, O_2/Ar gas of mixture 50/100 sccm and bias voltage of -75 V [13]. The obtained thickness of ZnO film is 3 μm. After deposition of the ZnO film on glass substrate, the wafer was patterned by photolithography using a positive photoresist (RZJ304) to form IDT electrode patterns. The patterned wafer was then put into the sputtering chamber for deposition of the AZO layer. Once completed, the wafer was immersed into acetone to remove photoresist and obtain the IDT electrodes. The distance between the two IDT transducers is 20 λ, where the wavelength, λ, is determined by the IDT pitch. The transmission (S_{21}) characteristics of the SAW devices were measured using an Agilent E5071C network analyzer.

RESULTS AND DISCUSSION

Figure 1(a) shows the XRD patterns of the AZO films deposited under different deposition pressure values with deposition power of 300 w, temperature of 200 ℃ and deposition time of 0.5 h. All the AZO films show a dominant XRD peak at $2\theta = 34.4°$, which corresponds to (0002) crystal orientation of the AZO. They are very close to that of the standard ZnO crystal (34.45°), independent of the Ar gas pressure. No Al_2O_3 phase was detected from the XRD patterns, indicating that all the Al atoms replace the zinc substitutionally in the hexagonal lattice, or Al segregate to the non-crystalline region in the grain boundary[14]. Based on Fig.1, with the increase of pressure, the intensity of the (0002) peak of AZO decreases, which is consistent with the literature [15]. The decreased intensity of the XRD indicates that more amorphous structure is present in the films. As increasing the deposition pressure leads to the decrease of kinetic energy of sputtered atoms and to a low surface mobility of the condensing species, especially at low deposition temperatures, the (0002) crystallization decreases when the pressure is increased. The lowest deposition pressure we used is 0.3 Pa, and this is because below this value, the glow discharge will become extinguished. Moreover, as the pressure increase the resistance decrease and the best resistivity of the AZO layers measured using the Van de Paul Hall measurement is about $4x10^{-4}$ Ω·cm, and the Hall mobility is 15.6 $cm^2/V·S^{-1}$, similar to most reported values [15].

Optical transmittance of the AZO films measured using the UV/visible spectrometer is shown in Fig. 1(b). The results show that the transparency of each AZO film is close to 90%, except the film deposited with a deposition pressure of 1.5 Pa. The high transparency demonstrates good quality of the AZO films.

Considering that the film with the deposition pressure of 0.3 Pa has the best the (0002) crystallization, lowest resistance as well as good optical transmittance, this paper use the deposition pressure of 0.3 Pa, with the deposition power of 300 w, temperature of 200 ℃ and deposition time of 0.5 h (750 nm).

Figure 2(a) is the schematic structure of the fabricated AZO/ZnO/Glass SAW devices. Figure 2(b) is an SEM picture of the AZO layer on top of ZnO layer of the device, showing a clear columnar structure with large grain size for both ZnO and AZO film, and the preferential c-axis orientation which is critical for high transparency and good performance SAW devices. Figure 2(c) shows the fabricated SAW devices on a glass wafer, showing a good transparency, by revealing clearly the background features. Figure 2(d) is Transmittance of the transparent SAW devices. Optical transmittance for the layered AZO/ZnO films on glasses was measured by a UV/visible spectrometer and it is over 80%.

The transmission (S_{21}) and the reflection (S_{11}) characteristics of the transparent SAW devices are shown in Fig. 3 (a)&(b). The first mode resonant frequency, f_1, was found to be 154.9 and 85 MHz, respectively, and the second mode resonant frequency, f_2, from 320 and to 175 MHz as the wavelengths of the IDTs was increased from 16 to 32 μm. A large signal amplitude up to about 25 dB was obtained for the first wave mode. These results clearly demonstrated that the transparent ZnO films have good piezoelectric effects, and the AZO layer functions well as the transparent electrodes. The amplitudes of the first mode resonance for all the devices are larger than the second mode resonance, implying the first mode resonance of the devices can be easily excited.

To study the effect of the series resistance of the IDT electrode on the performance of the transparent SAW devices, different resistance of AZO layers has been fabricated for transparent SAW devices. The spectrum results are shown in Fig.3(c). It is clearly show that when the sheet resistance of the AZO layer is larger than the 10 Ω/sq, the SAW performance is poor, indicating that to fabricate high performance SAW device, the sheet resistance of the electrode layer should be at least smaller than 10 Ω/sq.

To verify the vibration patterns of these two modes, we have performed simulation using the Finite Element Analysis (FEA) with commercial COMSOL 5.1 software in a two-dimensional (2D) piezo plane strain mode. The IDTs are periodic in nature, alternatively consisting of positive and negative potentials. Thus, one period of the electrode is sufficient to illustrate the performance of the SAW resonator. In this work, the experimental results of the transparent device (see Fig. 3(b)) with a wavelength of 32 μm were chosen for comparison with the simulation results. A model of an ZnO film with a thickness of 3 μm on a 60-μm thick glass substrate (about 2λ, thick enough for simulation, as the acoustic wave only penetrates into the substrate about one wavelength depth) was simulated with a fixed bottom boundary condition as shown in Fig. 4(a). A free and zero charge/symmetry boundary condition was assigned to the top surface of the piezoelectric ZnO layer. A polarization voltage value of 1 V was assigned to the 750 nm thick AZO electrode, while the other AZO electrode was assigned to be ground. The boundary between the ZnO and glass was assigned to be free and continuous. The two sides of the ZnO and glass substrate were assigned to be periodical boundary conditions. The material constants were extracted from the material library of COMSOL.

The simulation results are shown in Fig. 4(b). Clearly there are two large resonant peaks in the simulated frequency range which correspond to two SAW wave modes. The first peak is at 88.6 MHz, which corresponds to the experimental results of 85.0 MHz. Surface displacement, vibration and deformation of this mode are shown in Fig. 4(c), showing that the first peak is the Rayleigh wave-mode. Whereas the frequency of the second mode is 181.2 MHz from the simulation and the particle vibration analysis as shown in Fig. 4(c), confirming that the second wave mode is the Sezawa mode.

The phase velocity for the Rayleigh wave in an ideal (0002) ZnO layer is ~2650 m/s[17], depending on the crystal quality and deposition method used. The phase velocity for the Rayleigh wave in glass is 3200 m/s[18], which is larger than that of ZnO film. This is a layered structure, and the velocity of glass substrate is higher than that of ZnO film, thus it is expected to have a Sezawa resonance [19]. The Rayleigh phase velocities (v_p) of the

fabricated SAW devices ($v_p = \lambda f$) are 2478 and 2720 m·s^{-1}, respectively, increasing with the increased wavelength from 16 to 32 µm. When the wavelength is increased, more energy is dispersed in the glass substrate, leading to a higher velocity of the layered structure, consistent with the observation from other layered structure SAW devices[20]. The Sezawa phase velocity also increases from 5120 to 5600 m·s^{-1} with the wavelength increased from 16 to 32 µm, showing a similar trend with that of the Rayleigh wave.

It is well known that SAW devices can be used as sensors for monitoring changes of various physical parameters and micro-actuators for microfluidics and lab-on-chip. If transparent SAW devices can be proven to be useful for high performance sensors, this will open the door for widespread applications for inexpensive, transparent and invisible sensors and lab-on-a-chip for healthcare, medical research and environment monitoring. We have conducted temperature sensing experiments to show their suitability for sensing applications. Figure 5(a) shows the measure system of temperature sensor for transparent SAW device and Fig.5 (b) shows resonant frequency of the transparent SAW devices as a function of temperature. The temperature coefficients of frequency (TCF), defined as $\Delta f/\Delta T f_0$, are ~45 ppm/K for the wavelengths 16 µm.

When a liquid droplet is located on the path of the surface acoustic wave, the SAW will intact with liquid and the acoustic energy is coupled into the liquid, inducing acoustic streaming. The transparent SAW device developed in this study can also deliver the same functions, showing a stable streaming with a double vortex pattern with the signal voltage input. The measured streaming velocities increase with the increase of RF signal voltage applied to the IDT electrode or with the increase of droplet size, and reaches 2.27 cm s^{-1} at a signal voltage of 45 V and droplet size of 30 µL. The results showed that the transparent SAW devices can be used for transparent microfluidic, lab-on-chip applications.

CONCLUSIONS

In summary, we investigated characteristics of AZO thin films on glass substrates deposited by DC magnetron sputtering. Results show that a low deposition pressure will yield a good AZO film with (0002) orientation. We have fabricated the transparent SAW resonators on glass substrates using AZO as the electrodes using conventional UV-light photolithography and lift-off process. Transparent SAW devices with different wavelengths exhibited two wave modes of Rayleigh and Sezawa waves with good signal amplitude and high optical transmittance. The transparent SAW devices have demonstrated their ability to induce strong acoustic streaming and to sense temperature. This research demonstrated that transparent SAW devices have a great potential for applications in transparent electronics, microfludics, sensors and microsystems.

FIGURES

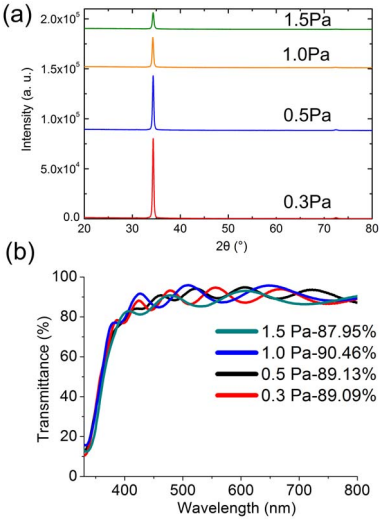

Figure 1: XRD patterns and Optical transmittance of the AZO films deposited under different deposition pressure values.

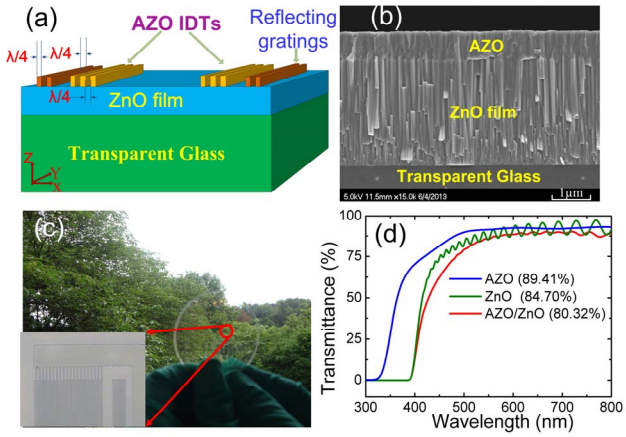

Figure 2:(a) A three-dimensional schematic of transparent SAW device; (b) SEM of the cross section of SAW device; (c) a photograph of a glass wafer with fabricated transparent SAW devices; (d) Transmittance of the transparent SAW devices.

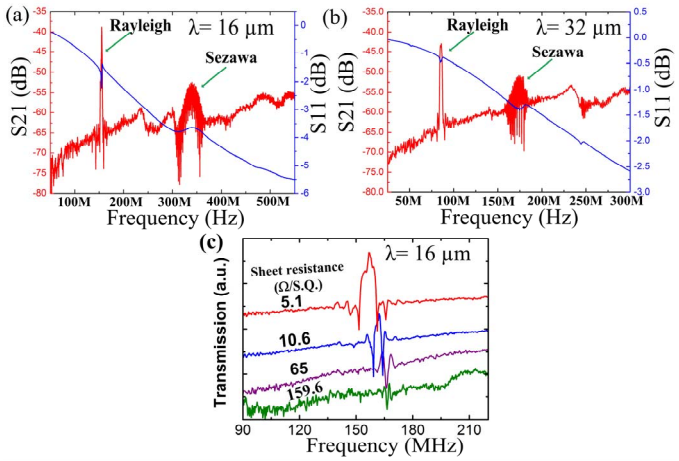

Figure 3: (a)&(b) Transmission spectrum of the transparent SAW devices as a function of wavelengths;(c) the effect of the sheet resistance of the AZO film on the resonant spectrum for a wavelength of 16 µm.

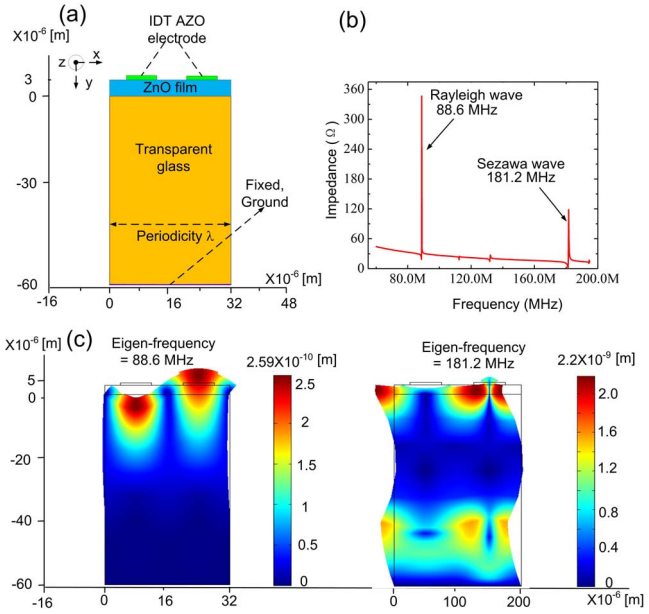

Figure 4: (a) Geometry of a periodic cell in the simulation; (b) simulated Impedance of the transparent SAW device and (c) particle vibration and surface deformation of the two modes.

.

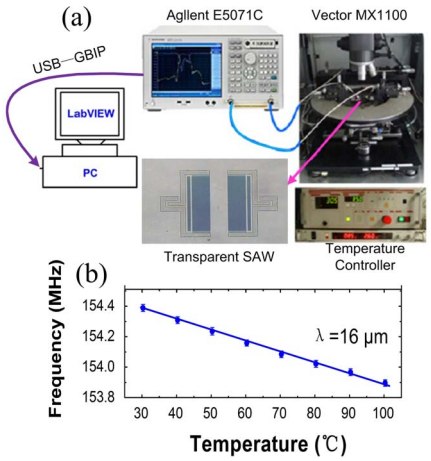

Figure 5:(a) The measure system of temperature sensor for transparent SAW device; (b) Resonant frequency decreases linearly with increase in temperature for the transparent SAW device.

ACKNOWLEDGEMENTS

This work was supported by the National Natural Science Foundation of China (Grant No. 51605485) and the National University of Defense Technology Research Project (No. ZK16-03-11).

REFERENCES

[1] S. Lee, A. Reuveny, J. Reeder, S. Lee, H. Jin, Q. H. Liu, et al., A transparent bending-insensitive pressure sensor, Nature Nanotech., vol. 11, pp. 472–478, 2016.

[2] H. Jang, Y.J. Park, X. Chen, T. Das, M.S. Kim, J.H. Ahn, Graphene-Based Flexible and Stretchable Electronics, Adv. Mater., vol. 28, pp. 4184-4202, 2016.

[3] T. Georgiou, R. Jalil, B.D. Belle, L. Britnell, R.V. Gorbachev, S.V. Morozov, et al., Vertical field-effect transistor based on graphene-WS_2 heterostructures for flexible and transparent electronics, Nature Nanotech., vol. 8, pp.100-103, 2013.

[4] M. Mativenga, D. Geng, B. Kim, J. Jang, Fully Transparent and Rollable Electronics, ACS Appl. Mater. Interfaces, vol. 7, pp. 1578-1585, 2015.

[5] K. Lee, W. Wang, T. Kim, S. Yang, A novel 440 MHz wireless SAW microsensor integrated with pressure-temperature sensors and ID tag, J. Micromech. Microeng., vol. 17, pp. 515, 2007.

[6] R. Fachberger, A. Erlacher, Applications of wireless SAW sensing in the steel industry, Procedia Eng, vol. 5, pp. 224-227, 2010.

[7] L.Y. Yeo, J.R. Friend, Surface Acoustic Wave Microfluidics, Annu. Rev. Fluid. Mech., vol. 46, pp. 379-406, 2014.

[8] M. Elm, T. Henning, P. Klar, B. Szyszka, Effects of artificially structured micrometer holes on the transport behavior of Al-doped ZnO layers, Appl. Phys. Lett., vol. 93, pp. 232101, 2008.

[9] J. Meyer, P. G. rrn, S. Hamwi, H-H Johannes, T. Riedl, W. Kowalsky, Indium-free transparent organic light emitting diodes with Al doped ZnO electrodes grown by atomic layer and pulsed laser deposition, Appl. Phys. Lett., vol. 93, pp. 073308, 2008.

[10] S. Gupta, A. Joshi, M. Kaur, Development of gas sensors using ZnO nanostructures, J. Chem. Sci., vol. 122, pp. 57-62, 2010.

[11] S. Jung, Y. Han, B. Koo, J. Lee, J. Joo, Low temperature deposition of Al-doped zinc oxide films by ICP-assisted reactive DC magnetron sputtering, Thin Solid Films, vol. 475, pp. 275-278, 2005.

[12] Z. Guo, H. Zhang, D. Zhao, Y. Liu, B. Yao, B. Li, et al., The ultralow driven current ultraviolet-blue light-emitting diode based on n-ZnO nanowires/i-polymer/p-GaN heterojunction, Appl. Phys. Lett., vol. 97, pp. 173508, 2010.

[13] J. Zhou, X. He, H. Jin, W. Wang, B. Feng, S. Dong, et al., Crystal structure effect on the performance of flexible ZnO/polyimide surface acoustic wave devices, J. Appl. Phys., vol. 114, pp. 04452.1-8, 2013.

[14] D. K. Kim, H. B. Kim, Room temperature deposition of Al-doped ZnO thin films on glass by RF magnetron sputtering under different Ar gas pressure, J. Alloys. Compd., vol. 509, pp. 421-425, 2011.

[15] D. Y. Song, A. G. Aberle, J. Xia, Optimisation of ZnO:Al films by change of sputter gas pressure for solar cell application, Appl. Surf. Sci., vol. 195, pp. 291–296, 2002.

[16] H. Sato, T. Minami, S. Takata,T. Mouri, N. Ogawa, Highly conductive and transparent ZnO:Al thin films prepared on high-temperature substrates by d.c. magnetron sputtering, Thin Solid Films, vol. 220, pp. 327-332, 1992.

[17] K. Kalantar-Zadeh, Y.Y. Chen, B.N. Fry, A. Trinchi, W. Wlodarski, A novel Love mode SAW sensor with ZnO layer operating in gas and liquid media, IEEE Proc. Ultrason. Symp., vol. 1, pp. 353-356, 2001.

[18] J. Fraser, B.T. Khuri-Yakub, G.S. Kino, The design of efficient broadband wedge transducers, Appl. Phys.

Lett., vol. 32, pp. 698-700, 1978.
[19] X.Y. Du, Y.Q. Fu, S.C. Tan, J.K. Luo, A.J. Flewitt, W.I. Milne, et al., ZnO film thickness effect on surface acoustic wave modes and acoustic streaming, Appl. Phys. Lett., vol. 93, pp. 094105.1-3, 2008.
[20] M. Kadota, C. Kondoh, Influence of step-like portions on the surface of ZnO/glass SAW filters on their frequency characteristics, IEEE Trans.Ultrason. Ferroelectr. Freq. Control, vol. 44, pp. 658-665, 1997.

CONTACT

*X.Z. Wu, tel: +86-13807318490; xzwu@nudt.edu.cn